Controlling the spectrum of light pulses by dynamical electromagnetically induced transparency

Emilio Ignesti,[1] Roberto Buffa,[2] Lorenzo Fini,[1,3] Emiliano Sali,[1,*] Marco V. Tognetti,[1] and Stefano Cavalieri[1,3]

[1]*Dipartimento di Fisica e Astronomia, Università di Firenze and CNISM, Via G. Sansone 1, I-50019 Sesto Fiorentino, Firenze, Italy*

[2]*Dipartimento di Fisica, Università di Siena and CNISM, Via Roma 56, I-53100 Siena, Italy*

[3]*European Laboratory for Non-Linear Spectroscopy (LENS), Università di Firenze, Via N. Carrara 1, I-50019 Sesto Fiorentino, Firenze, Italy*

(Received 30 December 2010; published 12 May 2011)

We present a theoretical and experimental study on the possibility of spectral manipulation of weak probe-laser pulses in the presence of dynamical electromagnetically induced transparency. We predict a spectral enlargement or narrowing process depending on whether the probe-laser pulse is overlapped by the rising or the falling edge of the coupling pulse, respectively. The results of an experiment in sodium atomic vapors confirm the theoretical predictions.

DOI: 10.1103/PhysRevA.83.053411 PACS number(s): 42.50.Gy, 42.50.Nn, 42.25.Bs, 31.15.ap

In recent years there has been great activity in the field of pulse propagation in coherently prepared atomic media. In addition to a fundamental interest toward a more thorough understanding of the basic laws of laser-matter interaction, the attention of the scientific community has been attracted by the possible future applications of these phenomena in the field of all-optical technologies. One of the schemes that was most studied and which has shown the greatest potentials is electromagnetically induced transparency (EIT) [1,2], in which an intense coupling field is used to control the propagation dynamics of a weak resonant probe pulse. Initially, particular attention was devoted to ultraslow light propagation and light storage techniques with narrow-band (≈MHz) laser pulses [3–5]. Subsequently EIT schemes were proposed and/or used to control other pulse characteristics. For example, spatiotemporal control over the pulses via coherent atomic memory has been demonstrated [6,7]. Also, EIT has been used to obtain large values of the delay-bandwidth product with broadband (≈GHz) laser pulses [8] or to control the central frequency of a laser pulse [9]. The possibility of controlling the temporal shape of laser pulses using EIT has been theoretically envisaged [10,11] and this last additional control has been used to compensate for distortion in an optical delay line based on EIT [12].

In this work we focus our attention on the possibility to control and modify the spectral bandwidth of laser pulses propagating in an EIT-modified medium. In the field of optical communications, the control over the spectral bandwidth would be desirable in view of an optical control over the characteristics of a transmission line. Moreover, a reduction of the spectral bandwidth could be of interest for *wavelength-division-multiplexing* applications.

The basic idea is to exploit the peculiarities of an EIT scheme where the probe pulse is overlapped by a time-dependent coupling field. We predict theoretically a spectral enlargement or narrowing process for an increasing or decreasing coupling pulse temporal profile, respectively. An experimental realization in sodium atomic vapors confirms our theoretical predictions.

Figure 1 shows a schematic diagram of our experimental setup and, in the top-left inset, of the employed ladder EIT scheme, consisting of three atomic levels in interaction with two laser pulses propagating along the direction z. The probe pulse, resonant with the 1–2 transition, propagates in a medium modified by the presence of the much stronger and longer coupling pulse, resonant with the 2–3 transition. We consider the case where the probe pulse is always overlapped by a coupling field with a constant time slope. We refer to the ascending and descending cases as those corresponding to the probe pulse overlapped by, respectively, the rising and the falling edge of the coupling pulse. The ascending case is schematically shown in the oscilloscope picture in Fig. 1. While keeping the formulation general, we have in mind the case of a medium consisting of sodium atomic vapors, where we actually made our experiments. In this case $|1\rangle = |2p^6\,3s,\ J = 1/2\rangle$, $|2\rangle = |2p^6\,3p,\ J = 1/2\rangle$, and $|3\rangle = |2p^6\,3d,\ J = 3/2\rangle$, and the wavelengths of the probe and the coupling fields are $\lambda_p = 2\pi c/\omega_p = 589.756$ nm and $\lambda_c = 2\pi c/\omega_c = 818.550$ nm, respectively. In this scheme the strong coupling field is unaffected by the atomic sample, while the evolution of the weak probe field envelope is governed by the following propagation equation:

$$\frac{\partial \Omega_p}{\partial z} = -i\frac{N\omega_p\, d_{12}^2}{2\hbar\,\epsilon_0\, c}\rho_{12}, \tag{1}$$

which is coupled to the following Liouville equation for the atomic coherences:

$$\begin{aligned}\frac{\partial \rho_{12}}{\partial \tau} &= -i\Omega_p - i\Omega_c\rho_{13} - \gamma_{12}\rho_{12},\\ \frac{\partial \rho_{13}}{\partial \tau} &= -i\Omega_c\rho_{12} - \gamma_{13}\rho_{13}.\end{aligned} \tag{2}$$

Here $\Omega_p = d_{12}E_p/2\hbar$ and $\Omega_c = d_{23}E_c/2\hbar$ are the Rabi frequencies of the probe and the coupling field, respectively, d_{ij} is the electric dipole moment of the $i - j$ transition, N is the atomic density, and we introduce the new variable $\tau = t - z/c$. In the frequency domain Eqs. (1) and (2) read as

$$\frac{\partial S_p}{\partial z} = -i\frac{N\omega_p\, d_{12}^2}{2\hbar\,\epsilon_0\, c}S_{12}, \tag{3}$$

$$\begin{aligned} i\omega S_{12} &= -iS_p - iS_c \otimes S_{13} - \gamma_{12}S_{12},\\ i\omega S_{13} &= -iS_c \otimes S_{12} - \gamma_{13}S_{13},\end{aligned} \tag{4}$$

*Corresponding author: sali@fi.infn.it

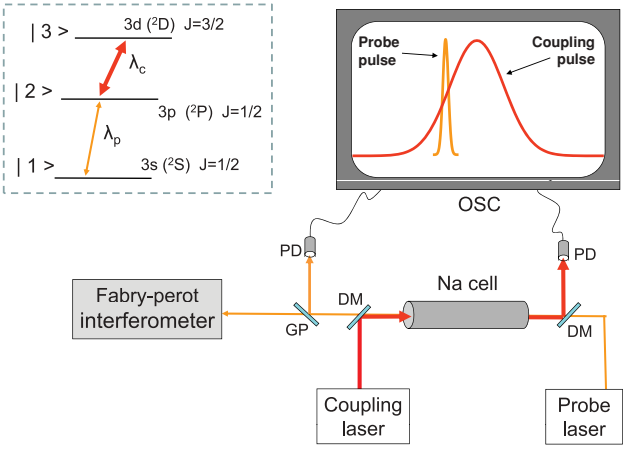

FIG. 1. (Color online) Scheme of the employed experimental apparatus. DM: dichroic mirror. GP: glass plate. PD: photodiode. OSC: digital oscilloscope. The picture in the oscilloscope shows a situation where the much shorter probe pulse is temporally overlapped with a part of the rising edge of the coupling pulse (ascending case) having an approximately constant slope. The vertical scales were normalized, as in fact the probe pulse is much weaker than the coupling pulse. Top left: diagram of the three sodium levels and the two laser fields involved in the proposed scheme.

where $S_p(z,\omega)$, $S_c(\omega)$, and $S_{1j}(z,\omega)$ are the Fourier transforms of $\Omega_p(z,\tau)$, $\Omega_c(\tau)$, and $\rho_{1j}(z,\tau)$, respectively, and $S_c(\omega)\otimes S_{1j}(z,\omega)$ is the convolution integral of $S_c(\omega)$ and $S_{1j}(z,\omega)$. An analytical simplification is obtained if we assume a constant control field slope. Then, expanding Ω_c to the first order in τ, i.e., $\Omega_c(\tau)=\Omega_{c0}(1+\alpha\tau)$, leads to

$$S_c=\Omega_{c0}\left[\delta(\omega)-i\alpha\frac{d}{d\omega}\delta(\omega)\right], \tag{5}$$

where $\delta(\omega)$ is the Dirac delta function.

Introducing now Eq. (5) into Eq. (4) we obtain

$$\begin{aligned}\alpha\frac{\partial S_{12}}{\partial\omega}\Omega_{c0}&=i\Omega_{c0}S_{12}+(i\omega+\gamma_{13})S_{13},\\ \alpha\frac{\partial S_{13}}{\partial\omega}\Omega_{c0}&=(i\omega+\gamma_{12})S_{12}+i\Omega_{c0}S_{13}+iS_p.\end{aligned} \tag{6}$$

For $\Omega_{c0}\gg\delta\omega_p\gg\alpha$, where $\delta\omega_p$ is the full-width at half-maximum (FWHM) spectral bandwidth of the probe pulse, it is possible to find an analytical solution to the coupled equations (3)–(6) [13]. This appears particularly straightforward in the limit case $\gamma_{12}=\gamma_{13}=0$, where it provides

$$S_p(L,\omega)=\frac{1}{m}S_p\left(0,\frac{\omega}{m}\right)\exp[i\phi(\omega)], \tag{7}$$

where

$$m=\exp\left(\frac{\omega_p\,d_{12}^2}{\hbar\,\varepsilon_0\,c}\frac{\alpha}{\Omega_{c0}^2}NL\right) \tag{8}$$

and

$$\phi(\omega)=\left[\exp\left(-\frac{\omega_p\,d_{12}^2}{\hbar\,\varepsilon_0\,c}\frac{\alpha}{\Omega_{c0}^2}NL\right)-1\right]\frac{\omega}{2\alpha}. \tag{9}$$

Directly from Eq. (7) it follows that the probe pulse FWHM spectral bandwidth $\delta\omega_p$ at the output the cell is given by

$$\delta\omega_p=m\delta\omega_{p0}, \tag{10}$$

where $\delta\omega_{p0}$ is the probe pulse spectral bandwidth at the cell input.

Equations (7) and (8) provide quite remarkable results. In particular, for constant coupling field ($\alpha=0$) the probe pulse spectral bandwidth remains unaffected ($m=1$), while in the ascending ($\alpha>0$) or descending ($\alpha<0$) case, the probe spectral bandwidth is enlarged ($m>1$) or compressed ($m<1$), respectively. The factor m results to be independent from any spectral profile of the probe pulse at the cell input. Also, Eq. (7) predicts that the probe pulse spectrum at the exit of the cell must have the same shape of that at the entrance.

This result was predicted by Fleischhauer and Lukin [7] and analyzed in terms of temporal variation of the group velocity of adiabatic dark-state polaritons. When the group velocity of the polaritons increases (decreases) in time, the spectral bandwidth of the light pulse decreases (increases). Our approach in the frequency domain confirms this interpretation. In fact, in the ascending (descending) case, the probe pulse experiences in its propagation an increasing (decreasing) intensity of the control field, which in turn determines a decrease (increase) of its propagation velocity, and an increase (decrease) of its spectral bandwidth.

Figure 2 shows the probe pulse spectrum predicted at the end of an atomic sodium sample of density-length product NL in the ascending (left column) and descending (right column) case. The spectral profile of the probe pulse for zero sodium

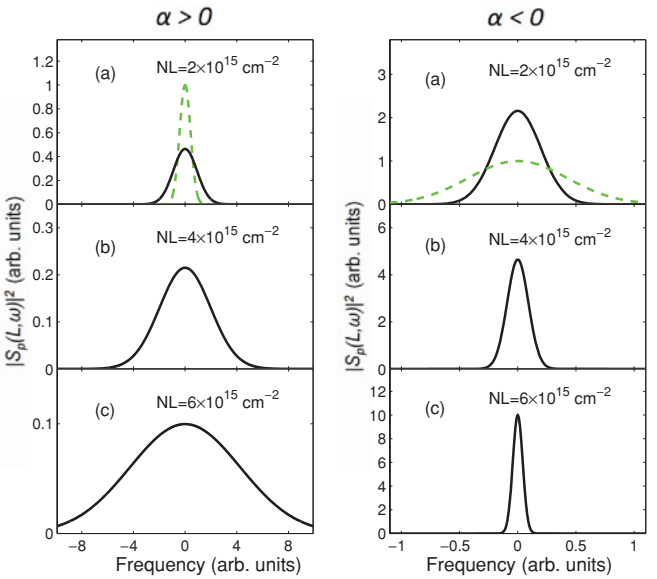

FIG. 2. (Color online) Probe pulse spectrum predicted by Eqs. (7) and (8) at the end of an atomic sodium sample of density-length product NL in the ascending (left column) and descending (right column) case. The spectral profile of the probe pulse upon entering the cell is reported in (a) as a dashed green line. The reported spectra correspond to various values of the density-length product NL, as indicated. The coupling field parameters $\Omega_{c0}/2\pi=8.8$ GHz and $\alpha=\pm3.7\times10^{-4}$ GHz are those of the coupling pulse actually used in the experiments.

density (i.e., in absence of EIT) is reported in (a) as a dashed green line. The reported spectra correspond to various values of the density-length product, as indicated [case (a) corresponds to the condition of our experiment]. The coupling field parameters $\Omega_{c0}/2\pi = 8.8\,\text{GHz}$ and $\alpha = \pm 3.7 \times 10^{-4}$ GHz are those of the coupling pulse actually used in the experiment (see below for details). The obtained spectral enlargement (compression) factors m are (a) 2.2 (0.45), (b) 4.7 (0.21), and (c) 10 (0.1).

The modification of the spectral bandwidth of the probe pulse cannot be the result of chirping of an ac Stark shift, since this cannot produce a spectral narrowing of the probe pulse but only a spectral broadening. Some more subtle effect is here at play, that is, the spectral mixing of the frequencies of the coherence ρ_{12}, source term for the propagation of the probe field. This frequency mixing is shown by the convolution integrals in Eq. (4).

The experimental apparatus employed is schematically shown in Fig. 1. The probe field is provided by a frequency-tunable multimode dye laser. The dye laser pulses have a measured average spectral bandwidth $\delta\omega_{p0}/2\pi = 1.7$ GHz and a duration of a few nanoseconds. The control field is provided by a frequency-tuneable, single-longitudinal-mode titanium-sapphire (Ti:S) laser [14] delivering smooth pulses with temporal FWHM equal to 60 ns. The measurements are carried out with a coupling pulse peak intensity equal to 40 kW/cm^2. These values of the experimental parameters satisfy the condition $\Omega_{c0} \gg \delta\omega_p \gg \alpha$ of the analytical model. The wavelength of the pulsed emission from the Ti:S laser is monitored using a wavelength meter with a resolution of 1 pm. Both lasers are pumped by a frequency-doubled Q-switched Nd:YAG laser. The two laser beams are linearly polarized along the same direction and they overlap, both temporally and spatially, inside the cell. A counterpropagating configuration is arranged for the purpose of reducing the effect of Doppler broadening. Portions of both pulses are detected by two photodiodes and the resulting signals are analyzed by a digital oscilloscope, in order to monitor the temporal synchronization of the two pulses (which can be changed by mutually adjusting the triggers of the two Nd:YAG pump lasers).

The sodium sample is contained in a cylindrical cell heated up to a temperature of 250°C for a length $L = 1$ m, corresponding to an independently measured density-length product $NL = 2 \times 10^{15}$ cm^{-2}. At the exit of the cell the probe pulse is spectrally analyzed by a Fabry-Perot interferometer [free spectral range (FSR) of 7.5 GHz], whose output signal is acquired by a PC and then processed to provide the probe pulse spectrum. The averaged probe-pulse spectrum at the output of the sodium cell is measured in the two different configuration in which the probe pulse is overlapped either by the rising or by the falling edge of the coupling pulse. The two pulses are arranged in such a way that the coupling pulse Rabi frequency temporal profile overlapping the probe pulse can be approximated as $\Omega_c(\tau) \approx \Omega_{c0}(1 + \alpha\tau)$, where $\Omega_{c0}/2\pi = 8.8\,\text{GHz}$ and $\alpha = \pm 3.7 \times 10^{-4}$ GHz are the values corresponding to the half-maximum of the coupling intensity in the leading and trailing edges, respectively.

Figure 3 reports the measured averaged spectra (black solid lines) in the three cases, i.e., with zero sodium density (absence of EIT) (a), and with a density-length product $NL =$ 2×10^{15} cm^{-2} in the ascending (b) and in the descending (c) case. This experimental condition corresponds to the theoretical situation reported in Fig. 2(a). In all cases the spectrum is centered at the zero value of the frequency axis and its maximum value is normalized to 1. The FWHM widths of the three spectra are, respectively, $\delta\omega_p/2\pi = (1.7 \pm 0.2)$ GHz, $\delta\omega_p/2\pi = (3.9 \pm 0.3)$ GHz, and $\delta\omega_p 2\pi = (0.6 \pm 0.1)$ GHz. The good agreement between theoretical predictions of Eq. (10) and experimental results is immediately evident from this figure, that is, the probe-pulse spectrum gets broader when the pulse is overlapped by the rising edge of the coupling pulse ($\alpha > 0, m > 1$), while it gets narrower when overlapped by the falling edge of the coupling pulse ($\alpha < 0, m < 1$). In (b) and (c) the dashed red curve represents the spectrum without the presence of EIT [as in Fig. 3(a)] scaled by the relevant

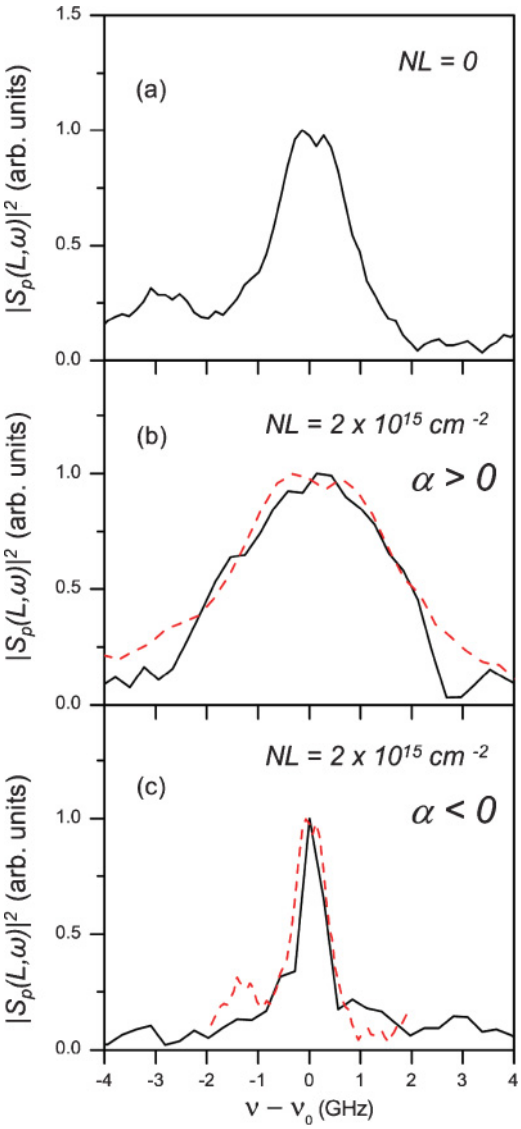

FIG. 3. (Color online) Averaged probe pulse spectral profile (black solid lines) measured (a) for negligible sodium density and at the output of a sodium cell in (b) the ascending and (c) descending case (ν_0 is the center of each spectrum). In (b) and (c) the dashed red curve represents the spectrum reported in (a) scaled by the relevant theoretical enlargement or compression factors (see text).

TABLE I. Values of m obtained theoretically and experimentally using a sodium density-length product $NL = 2 \times 10^{15}$ cm^{-2} in the ascending ($\alpha > 0$) and the descending ($\alpha < 0$) case.

	Theoretical	Experimental
$\alpha > 0$	2.2	2.3 ± 0.4
$\alpha < 0$	0.45	0.35 ± 0.10

theoretical enlargement or compression factors. Inspection of these figures visually confirms the good agreement between theory and experiment also from a quantitative point of view.

A concise quantitative comparison between theory and experiment can be realized by comparing the spectral enlargement or compression factors obtained experimentally, i.e., the ratios of the FWHM bandwidth values measured experimentally, with the predicted values of m, which for the relevant experimental parameters (density length product $NL = 2 \times 10^{15}$ cm^{-2}) are $m = 2.2$ for the case of the enlargement and $m = 1/2.2 \simeq 0.45$ for the case of the compression. This comparison is shown in Table I, where the good quantitative agreement between the experimental results and the predictions of the theory [Eq. (10)] is evident. It is important to note that the comparisons between theory and experimental data shown in Fig. 3 and Table I are made without free parameters.

In summary, we studied a three-level scheme for spectral manipulation of weak laser pulses, obtained exploiting the peculiarities of pulse propagation in the presence of dynamical electromagnetical induced transparency, i.e., for a time-dependent coupling field. We theoretically predicted that a spectral enlargement or compression process occurs when the probe pulse is overlapped by a coupling field with a positive or negative temporal slope, respectively. The experimental results that we obtained for a scheme in sodium atomic vapors are in very good agreement with our theoretical predictions, both qualitatively and quantitatively. In the field of optical communications, the possibility to control the spectral bandwidth of a light pulse might be of interest in view of an optical control over the parameters of a transmission line. We also envisage applications of this scheme to the vacuum ultraviolet spectral region (using different atomic samples), where at present this technique appears as unique for spectral manipulation of laser pulses.

[1] S. E. Harris, Phys. Today **50**, 36 (1997).
[2] M. Fleischhauer, A. Imamoglu, and J. P. Marangos, Rev. Mod. Phys. **77**, 633 (2005).
[3] L. V. Hau, S. E. Harris, Z. Dutton, and C. H. Behroozi, Nature (London) **397**, 594 (1999).
[4] D. F. Phillips, A. Fleischhauer, A. Mair, R. L. Walsworth, and M. D. Lukin, Phys. Rev. Lett. **86**, 783 (2001).
[5] Chien Liu, Z. Dutton, C. H. Behroozi, and L. V. Hau, Nature (London) **409**, 490 (2001).
[6] M. D. Eisaman, L. Childress, A. André, F. Massou, A. S. Zibrov, and M. D. Lukin, Phys. Rev. Lett. **93**, 233602 (2004).
[7] M. Fleischhauer and M. D. Lukin, Phys. Rev. A **65**, 022314 (2002).
[8] E. Ignesti, S. Cavalieri, L. Fini, E. Sali, R. Eramo, M. V. Tognetti, and R. Buffa, Phys. Rev. A **80**, 011811(R) (2009).
[9] E. Ignesti, R. Buffa, L. Fini, E. Sali, M. V. Tognetti, and S. Cavalieri, Phys. Rev. A **81**, 023405 (2010).
[10] R. Buffa, S. Cavalieri, and M. V. Tognetti, Phys. Rev. A **69**, 033815 (2004).
[11] V. G. Arkhipkin and I. V. Timofeev, Phys. Rev. A **73**, 025803 (2006).
[12] I. Novikova, D. F. Phillips, and R. L. Walsworth, Phys. Rev. Lett. **99**, 173604 (2007).
[13] E. Ignesti, R. Buffa, L. Fini, E. Sali, M. V. Tognetti, and S. Cavalieri (to be published).
[14] E. Sali, E. Ignesti, S. Cavalieri, L. Fini, M. V. Tognetti, and R. Buffa, Opt. Commun. **282**, 3330 (2009).